Dynamic Mode Decomposition of wake flow: reconstruction and performance metrics

Mustafa Hicret Yaman[1] and Gamze Yuksel[2]

[1]Department of Mathematics, Faculty of Science, Mugla Sitki Kocman University, 48000, Mugla, Turkiye.
[2]Department of Mathematics, Faculty of Science, Mugla Sitki Kocman University, 48000, Mugla, Turkiye.
E-mail: mhicretyaman@mu.edu.tr[1], ngamze@mu.edu.tr[2]

Abstract

In this study, Dynamic Mode Decomposition (DMD) was used to analyze a turbulent wake flow around a cylindrical obstacle. Open-source OpenFOAM software was used to simulate the flow and generate the dataset. By using the created dataset and image processing, the model created with the DMD algorithm, state estimation and future state prediction of the flow were performed. The performance of the model was measured with performance metrics. These are Root Mean Square Error (RMSE) and Structural Similarity Index (SSIM) metrics. As a result of the analysis, it was observed that the model made consistent predictions.

2010 Mathematics Subject Classification. . 37N10, 37N30, 37M10, 37M05, 62R07, 68T09, 76D05, 94A08 .
Keywords. Computational fluid dynamics, Dynamic mode decomposition, Reduced order model, Machine Learning, Wake flow.

1 Introduction

Dynamic mode decomposition (DMD) is a mathematical method for analyzing the dynamic behavior of systems. It is a data-driven technique that can be used to identify patterns and modes of oscillation in a system, as well as to predict how the system will evolve over time. DMD is based on the concept of decomposing a system's behavior into a set of modes, each of which corresponds to a distinct pattern of oscillation. To perform DMD on a system, one must first collect time-series data on the system's behavior. This data is then used to construct a matrix that represents the system's dynamics. DMD is then applied to this matrix to identify the system's modes and to predict its state or future behavior.

One of the key advantages of DMD is that it can be applied to a wide range of systems, including those that are nonlinear, time-varying, or high-dimensional. It can also be used in conjunction with other mathematical techniques, such as control theory and machine learning, to further analyze and understand a system's behavior. Overall, DMD is a powerful tool for analyzing the dynamics of complex systems and for predicting their future behavior. It has been applied in a variety of fields, including engineering, physics, biology, and finance. Dynamic Mode Decomposition (DMD) is a mathematical algorithm for decomposing a complex system into a set of simpler, interconnected components or modes. DMD is a data-driven method that uses a time series of data from the system being studied to identify the underlying modes and their dynamics.

The DMD approach, which decomposes complex flows into simpler representations based on spatio-temporal coherent structures, was developed in the field of fluid dynamics. Schmid and Sesterhenn both provided examples of how the DMD algorithm may make predictions from high dimensional fluid data in [2, 1]. Due to its data-based, equation-free nature and its capacity to decompose complicated systems into spatio-temporally coherent structures that may be used for

Advanced Studies: Euro-Tbilisi Mathematical Journal 16, supplement issue 4 (2023), pp. 67–78.
DOI: 10.32513/asetmj/1932200823407
Tbilisi Centre for Mathematical Sciences.
Received by the editors: 18 November 2022.
Accepted for publication: 22 June 2023.

state prediction and control, DMD has grown in popularity. Mezic et al. [3, 4, 5] and Rowley et al. [6] have demonstrated in fundamental studies that may serve as the foundation for the theory of DMD that DMD is related to nonlinear dynamics through the Koopman operator theory [7] and can be interpreted using regular dynamic system techniques. DMD can be conceived of as a combination of spatial dimensionality reduction methods like proper orthogonal decomposition (POD) and temporal Fourier transformations. The usual method for calculating POD is singular value decomposition (SVD). It is also known as principal component analysis (PCA) in [8, 9]. DMD has a variety of applications and implications. Three main functions are typically attributed to the DMD algorithm.

Identification: Initially, complex fluid flows were described using the DMD algorithm as a diagnostic tool in [2, 6]. In many application domains, this can be DMD's main purpose. Similar to POD, the diagnostic structure of DMD enables data-based discovery of underlying structures in complicated systems.

State estimation and future state prediction: DMD is concerned with creating dynamic models of fundamental processes that have been observed using the dominating spatiotemporal structures in the data. This challenge is made more challenging by the fact that DMD is restricted to building the linear dynamic system that best fits (minimizes least squares) the nonlinear dynamic system that generates the data. As a result, the objective is to forecast the status of the system in a regime without measurements, as opposed to diagnosing.

Control: In this situation, the DMD algorithm enables a fully data-based approach to control theory and offers a demanding mathematical foundation for controlling complicated dynamic systems that are difficult to characterize in terms of unknowable or computationally difficult governing equations.

In this study, the DMD algorithm is used to perform Identification, state estimation and future state prediction of the flow. Then the performance of the model was measured with performance metrics.

2 Methodology

2.1 Dynamic Mode Decomposition

DMD is a method used to extract coherent fundamental structures from data. It can be seen as an ideal combination of temporal Fourier transforms with spatial POD techniques. DMD constructs the most appropriate linear dynamic system for the nonlinear dynamic system that generates the data in [10].

The DMD method is examined below. In the method, the time evolution of the variable being considered in the dynamic system is given by an ordinary differential equation, independent of the governing equation of the system;

$$\frac{d\boldsymbol{x}}{dt} = f(\boldsymbol{x}, t; \mu) \tag{2.1}$$

Here, the dynamic system's position at time t is represented by the vector $x(t)$, its parameters are represented by μ, and the dynamics are represented by f. The discrete form of the dynamic system given by Eq.(2.1) in continuous form is as follows:

$$\boldsymbol{x}_{k+1} = F(\boldsymbol{x}_k) \tag{2.2}$$

In the DMD method; Eq.(2.1) can be modeled as linear ordinary differential equation as follows:

$$\frac{d\boldsymbol{x}}{dt} = \mathrm{A}\boldsymbol{x} \tag{2.3}$$

where the initial condition is $\boldsymbol{x}(0)$. The solution of Eq.(2.3) is given below;

$$\boldsymbol{x}\,(t) = \sum_{k=1}^{n} \varphi_k e^{\omega_k t} b_k = \boldsymbol{\Phi} e^{\boldsymbol{\Omega} t} \boldsymbol{b} \tag{2.4}$$

ω_k and φ_k are the eigenvalues of the matrix A and their corresponding eigenvectors, respectively, and b_k is the coordinates of $x(0)$ based on the eigenvectors.

2.2 DMD algorithm

To apply the DMD algorithm, flow field data were obtained from the numerical simulation. The dataset is then split into two dataset separated by a sampling time step Δt, such that

$$\boldsymbol{X} = \begin{bmatrix} \vdots & \vdots & & \vdots \\ x_1 & x_2 & \cdots & x_{m-1} \\ \vdots & \vdots & & \vdots \end{bmatrix} \tag{2.5}$$

$$\boldsymbol{X'} = \begin{bmatrix} \vdots & \vdots & & \vdots \\ x_2 & x_3 & \cdots & x_m \\ \vdots & \vdots & & \vdots \end{bmatrix} \tag{2.6}$$

where $x_k \in \mathbb{C}^n$ is the k th snapshot of the flow field, m is the number of snapshots and the number of nodes in each snapshot is n [2, 10]. A linear mapping connecting $\boldsymbol{X'}$ and $\boldsymbol{X}$ is assumed to be

$$\boldsymbol{X'} \approx A\boldsymbol{X} \tag{2.7}$$

where A is a best-fit linear operator. Calculating A in a linear system is simple, but for a nonlinear system, an explicit computation of A can be very costly, especially on large datasets. For this reason, first the similarity matrix is derived and then the singular value decomposition (SVD) is applied.

$$A = \boldsymbol{X'}\boldsymbol{X}^{+} \tag{2.8}$$

where + is the Moore-Penrose pseudoinverse. In application, analyzing matrix A directly is difficult because the state size (n) is very large, so the economic SVD is applied: instead of decomposing matrix A, the low rank $\tilde{A}$ projected with proper orthogonal decomposition (POD) is calculated.

$$\boldsymbol{X} \approx \boldsymbol{U}\boldsymbol{\Sigma}\boldsymbol{V}^{*} \tag{2.9}$$

* represents conjugate transpose, $\boldsymbol{U} \in \mathbb{C}^{n\times r}$, $\boldsymbol{\Sigma} \in \mathbb{C}^{r\times r}$, $\boldsymbol{V} \in \mathbb{C}^{m\times r}$ and r represents the truncation rank of r-SVD. $\boldsymbol{\Sigma}$ contains non-zero singular values so it is diagonal matrix, $\boldsymbol{U}$ and $\boldsymbol{V}$ are both orthogonal. Also, A matrix

$$\boldsymbol{A} = \boldsymbol{X'}\mathbf{V}\boldsymbol{\Sigma}^{-1}\boldsymbol{U}^{*} \tag{2.10}$$

Then, to replace the full order matrix A, projected matrix $\tilde{A}$ can be constructed by minimizing the frobenius norm

$$\|\boldsymbol{X'} - \boldsymbol{AX}\|_F \tag{2.11}$$

which is

$$\|\boldsymbol{X}\|_F = \sqrt{\sum_{j=1}^{n}\sum_{k=1}^{m} \boldsymbol{X}_{jk}^2} \tag{2.12}$$

Then A matrix can be obtained by $\tilde{A}$

$$\tilde{A} = \boldsymbol{U}^* \boldsymbol{AU} = \boldsymbol{U}^* \boldsymbol{X'} \mathbf{V} \boldsymbol{\Sigma}^{-1} \tag{2.13}$$

$$A = \boldsymbol{X'} \mathbf{V} \boldsymbol{\Sigma}^{-1} \boldsymbol{U}^* \tag{2.14}$$

Next, eigendecomposition of A can be computed so that

$$\boldsymbol{AW} = \boldsymbol{W\Lambda} \tag{2.15}$$

where the diagonal matrix Λ consisting of the W eigenvectors and λ_k eigenvalues. The DMD modes can then be achieved via

$$\boldsymbol{\Phi} = \boldsymbol{X'} \mathbf{V} \boldsymbol{\Sigma}^{-1} \boldsymbol{W} \tag{2.16}$$

This equality is obtained when $\lambda_k \neq 0$, if $\lambda_k = 0$ then the equality became that $\boldsymbol{\Phi} = \boldsymbol{UW}$. Furthermore, the future state prediction is obtained by substituting Φ and Λ in equation (2.4).

2.3 Numerical model and simulation details

In this study, the behavior of the fluid flowing around a cylindrical obstacle that is stationary in a rectangular region is investigated. While producing the dataset, the open source OpenFOAM platform, which has been very popular recently in computational fluid Dynamics was used. The simplefoam solver that solves incompressible steady state turbulent flows is used in the model. Details of the solver are given below:

The algorithm solves the continuity equation:

$$\nabla \cdot \boldsymbol{u} = 0 \tag{2.17}$$

and the momentum equation:

$$\nabla \cdot (\boldsymbol{u} \otimes \boldsymbol{u}) - \nabla \cdot R = -\nabla p + S_u \tag{2.18}$$

where u is velocity, p is kinematic pressure, R is Stress tensor and S_u is Momentum source.

Description of computational domain and grid system in Figure 1 and Figure 2 below;

Inlet velocity $u = 0.06\ \frac{m}{s}$, Kinematic Viscosity $\nu = 1.5 \times 10^{-5}\ \frac{m^2}{s}$ and Reynolds number $Re = 200$.



FIGURE 1. Computational Domain

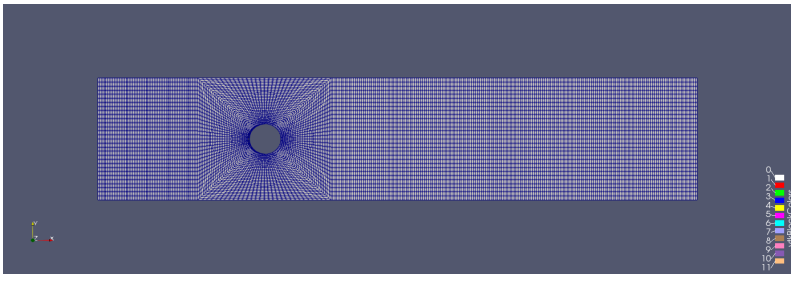


FIGURE 2. Domain Grid

The 30^{th}, 60^{th} and 90^{th} snapshots of the flow are given in Figure 3-5, respectively, below.

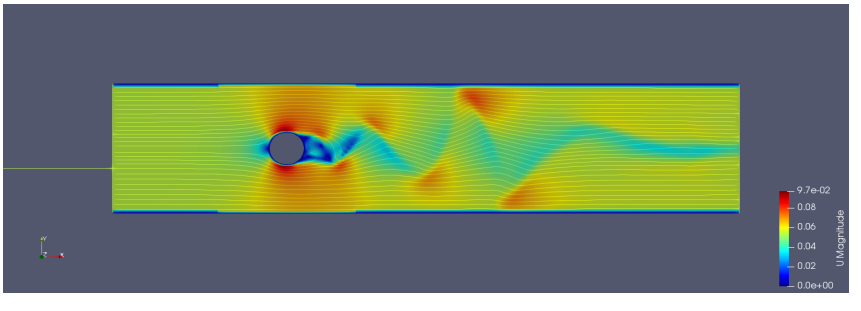


FIGURE 3. 30^{th} snapshot

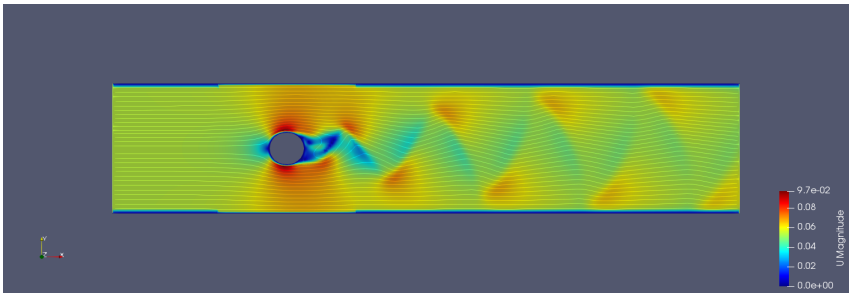


FIGURE 4. 60^{th} snapshot

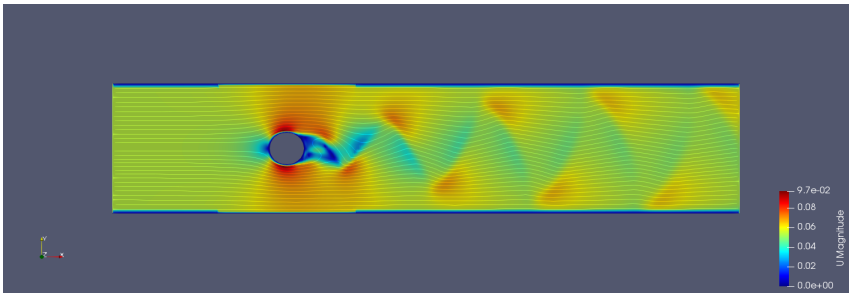


FIGURE 5. 90^{th} snapshot

2.4 Performance metrics

Two metrics were used to evaluate the performance of the model. These are Root Mean Square Error (RMSE) and Structural Similarity Index (SSIM). Details are given as below.

RMSE:
The RMSE is used to quantify the disparity between the original and reconstructed images, and the lower the RMSE number, the more accurate the model is.

$$\sqrt{\frac{\sum_{i=1}^{M}\sum_{j=1}^{N}|R(i,j)-O(i,j)|^2}{M\times N}}$$

where M and N are size of the image, i and j are the pixel coordinates in the image. R(i,j) is the reconstructed image and O(i,j) is the original image.

SSIM:
SSIM is a metric that is used to assess how similar two provided images are to one another. Luminance, contrast, and structure are the three main properties that the Structural Similarity Index measure pulls from an image. These three elements serve as the foundation for the comparison between the two photos. Also SSIM chart is given in Figure 6.

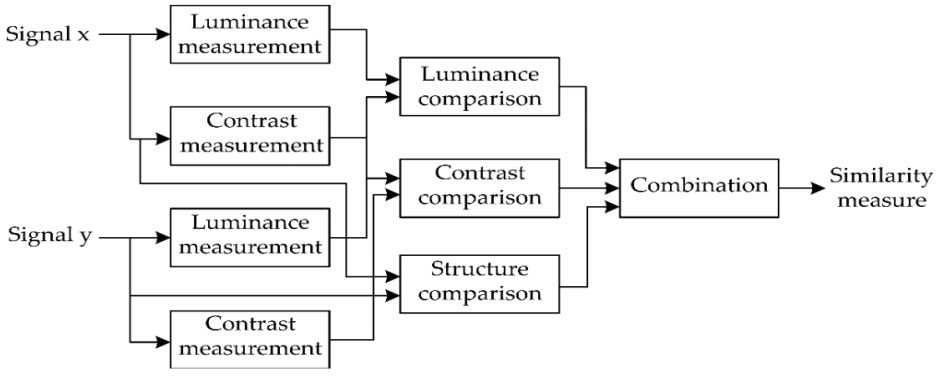


FIGURE 6. SSIM algorithm

And the following definition of the formula for the SSIM between a test signal y and a reference signal x as follows

$$SSIM\,(x,y) = [l(x,y)]^{\alpha}[c(x,y)]^{\beta}[s(x,y)]^{\gamma}$$

where $l(x,y)$ denotes the luminance, $c(x,y)$ denotes the contrast and $s(x,y)$ is the structure component. The parameters α , β , $\gamma > 0$ denote a weighted combination of the aforementioned components [11, 12].

3 Result and discussion

In this study, an incompressible turbulent flow around a cylindrical obstacle is investigated. Snapshots of the flow were produced by making calculations with the Simplefoam solver. Thus, 100 snapshots of the flow model were produced with the OpenFOAM platform and the dataset was created. Some sample images of the dataset are given in the previous section.

First of all, the state estimation was made by applying DMD to the created dataset. 30^{th}, 60^{th} and 90^{th} original snapshots and reconstructed snapshots are given in Figure 7a below:

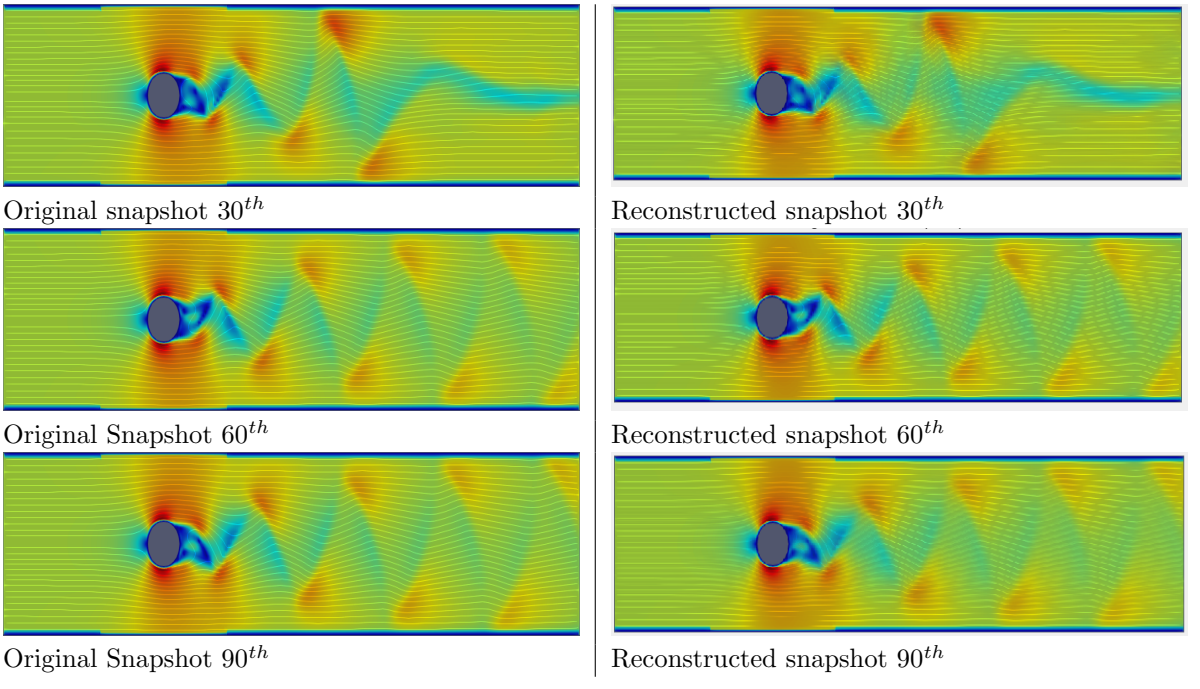


Figure 7a. Original and Reconstructed Images

Examining the original images and the reconstructed images of each snapshot (Table 3), it can be observed that the reconstructed images match the originals almost exactly. In addition to this, the performance metrics of the images reconstructed by the model trained on 100 images are given below.

RMSE values of the model for each Snapshot are given in Figure 7

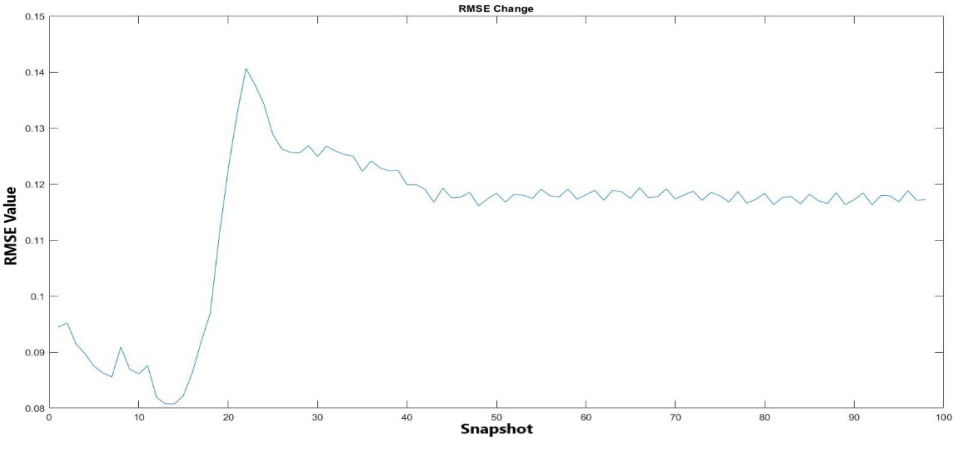


FIGURE 7. RMSE values of each snapshot

SSIM values of the model for each Snapshot are given in Figure 8

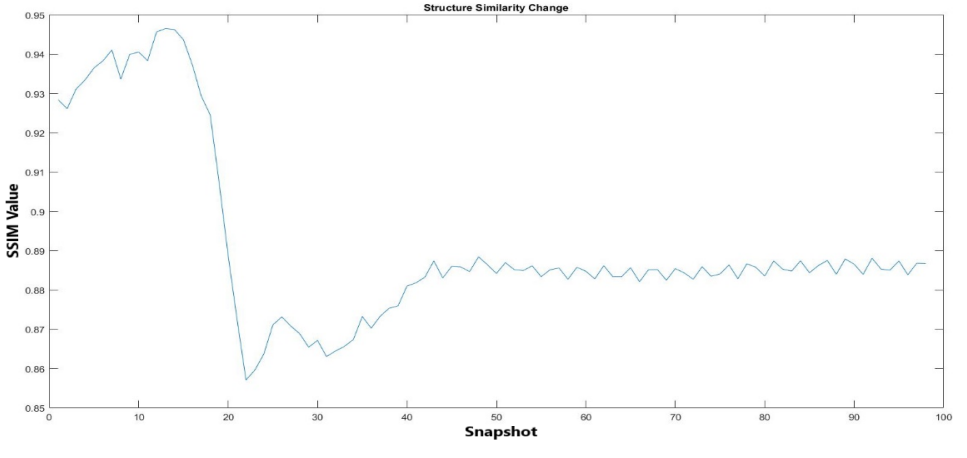


FIGURE 8. SSIM values of each snapshot

When the graphs of RMSE and SSIM metrics (Figure 7-8) are examined, there is a small decrease in performance as expected until the periodicity in the flow occurs (approximately between the 15th and 20th images), and then the performance increases and consistent results can be seen in the RMSE and SSIM metrics.

Furthermore, the model was trained with first 95 snapshots and then future-state prediction was performed; The model created the 96th (+1 time step), 97th (+2 time step) and 98th (+3 time

step) snapshots by training with the first 95 images and predicting them.
Figure 9 is given below, it consists of three sets of images. The left images are the original images, the right images are the future-state prediction of the original ones.

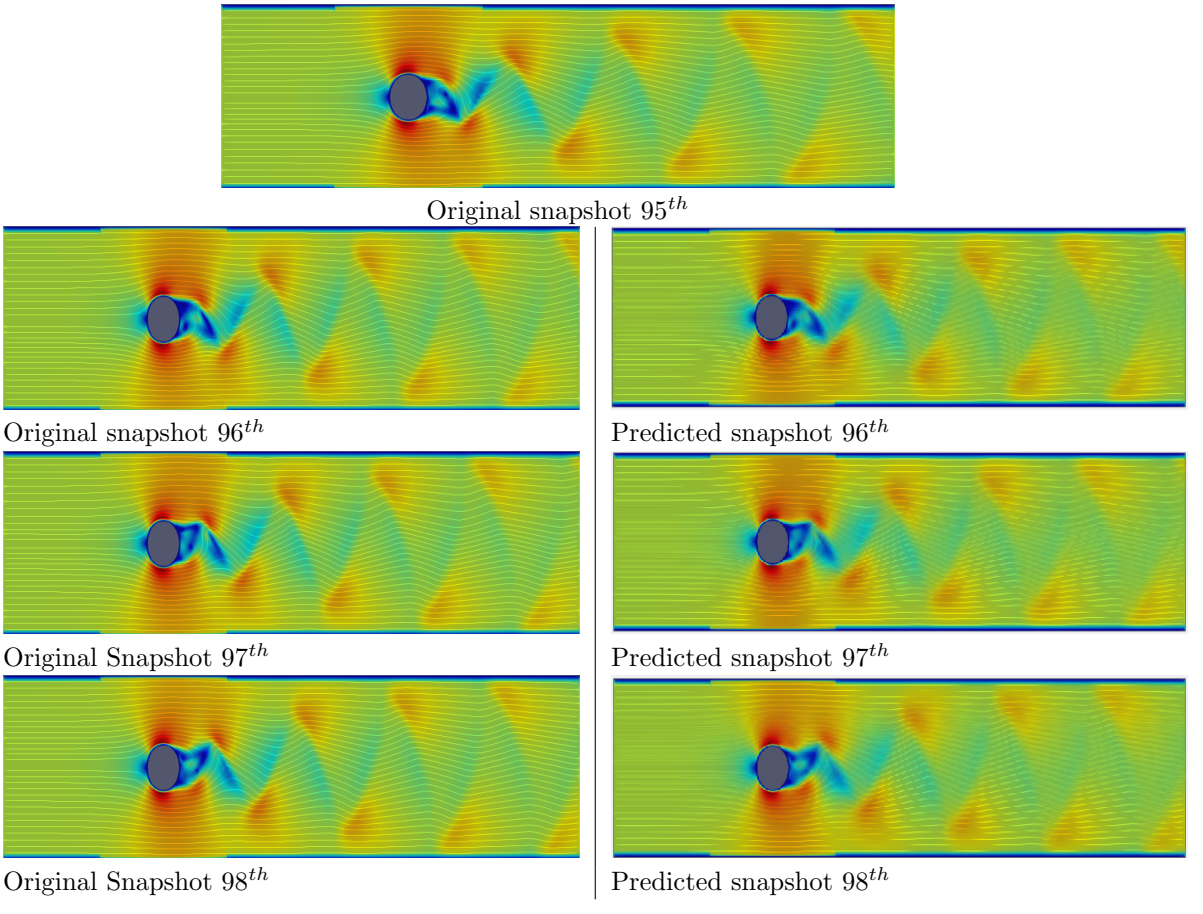


Figure 9. Originals and Predicted Images

The Table 1 containing the values of RMSE and SSIM, the performance metrics of the model for the future state predictions, is given below.

Snapshot	RMSE	SSIM
$96^{th}(+1)$	0.1111	0.9240
$97^{th}(+2)$	0.1201	0.8807
$98^{th}(+3)$	0.1305	0.8804

Table 1. Performance metrics of future-state prediction

When the images obtained for the future state prediction are examined, it is seen that the images are almost exactly compatible with the originals, as in the state estimation. If the performance metrics of the model's future predictions are evaluated, RMSE and SSIM; The model performs quite well in future-state prediction, and as the predicted time step grows, there has been a consistent decline in both RMSE and SSIM performances as expected.

Acknowledgement

This article is produced from the first author's dissertation as titled "Dynamic mode decomposition of fluid flows".
Furthermore, the preliminary work of this article is presented at the "ICMME 2022"

References

[1] P. J. Schmid and J. Sesterhenn, *Dynamic mode decomposition of numerical and experimental data*, In 61st Annual Meeting of the APS Division of Fluid Dynamics. American Physical Society, (2008).

[2] P. J. Schmid, *Dynamic mode decomposition of numerical and experimental data*, Journal of Fluid Mechanics, **656**(2010), 5–28.

[3] I. Mezic, *Spectral properties of dynamical systems, model reduction and decompositions*, Nonlinear Dynamics, **41**(2005), 309–325.

[4] I. Mezic and A. Banaszuk, *Comparison of systems with complex behavior*, Physica D: Nonlinear Phenomena, **197**(2004), 101–133.

[5] I. Mezic, *Analysis of fluid flows via spectral properties of the Koopman operator*, Annual Review of Fluid Mechanics, **45**(2013), 357–378.

[6] C. W. Rowley, I. Mezic, S. Bagheri, P. Schlatter and D. S. Henningson, *Spectral analysis of nonlinear flows, Journal of Fluid Mechanics*, **645**(2009), 115–127.

[7] B. O. Koopman, *Hamiltonian systems and transformation in Hilbert space*, Proceedings of the National Academy of Sciences of the USA, **17**(1931), 315–318.

[8] K. Pearson, *On lines and planes of closest fit to systems of points in space*, Philosophical Magazine, **2**(1901), 559–572.

[9] I. Jolliffe, *Principal Component Analysis*, Encyclopedia of Statistics in Behavioral Science, **3**(2005), 1580–1584.

[10] J. N. Kutz, S. L. Brunton, J. L. Brunton, J. L. Proctor, *Dynamic Mode Decomposition: Data-Driven Modeling of Complex Systems*, SIAM, 2016

[11] L. Sevcik, M. Voznak, J. Frnda, *QoE Prediction Model for Multimedia Services in IP Network Applying Queuing Policy*, In: 17th International Symposium on Performance Evaluation of Computer and Telecommunication Systems (SPECTS) part of SummerSim Multiconference, (2014), 593-598.

[12] J. Frnda, J. Nedoma, J. Vanus, R. Martinek, *A Hybrid QoS-QoE Estimation System for IPTV Service*, Electronics,**8**(2019), 585.

[13] J. Frnda, M. Durica, M. Savrasovs, P. Fournier-Viger and J. Lin, *QoS to QoE Mapping Function for Iptv Quality Assessement Based on Kohonen Map: A Pilot Study*, Transport and Telecommunication Journal,**21**(2020), 181-190.